

# MIMO RF PROBE FOR WIDE-AREA INDOOR HUMAN MOTION MONITORING

Chi Xu and Jeffrey Krolik

Department of Electrical and Computer Engineering, Duke University, Durham, NC 27708  
chi.xu@duke.edu, jk@ee.duke.edu

## ABSTRACT

This paper addresses the problem of RF-based wide-area human motion monitoring in indoor multipath environments. A major challenge for conventional pulse-Doppler radar in multipath scenarios is the difficulty in discriminating direct-path targets from ghost returns due to multipath scattering. In this paper, the ability of a multiple-input multiple-output (MIMO) RF probe to discern both direction-of-departure (DoD) and direction-of-arrival (DoA) via “non-causal” beamforming is exploited for indoor motion monitoring. Preliminary results with real data are presented which demonstrate the sidelobe suppression and multipath mitigation achieved. Also, MIMO processing is analyzed using the bi-directional beampattern and spectrum defined herein.

**Index Terms**— MIMO, wide-area, beamforming, sidelobe suppression, multipath mitigation

## 1. INTRODUCTION

Stand-off measurements of human motions is an important function in numerous applications such as public surveillance, human-computer interfaces, gait analysis, and patient diagnostics [1, 2]. Existing approaches can be classified into two main categories: Video-based and RF-based. Computer vision methods based on spatial-temporal features have been used for classifying human activities such as walking, jogging, running, jumping and so on, but are degraded by occlusions and less-than-ideal illuminations, as often occurs in wide-area indoor environments. In principle, RF-based methods can operate under all lighting conditions and are robust to occlusions, including walls. While the micro-Doppler signature has been used for classification purposes when the target is line-of-sight (LOS) and uncluttered by multipath returns, wide-area indoor applications require the ability to deal with, if not exploit, non-line-of-sight (NLOS) multipath propagation.

Multiple-input multiple-output (MIMO) radar has been used for separating multipath returns in over-the-horizon radar (OTHR) [3, 4] and ground moving target indicator (GMTI) [5–7]. The key advantage of MIMO over traditional single-input multiple-output (SIMO) systems in multipath environments is the ability to discriminate both direction-

of-departure (DoD) and direction-of-arrival (DoA) via the so-called “non-causal” beamforming [3, 4]. In this paper, a new application of MIMO is proposed: wide-area indoor motion monitoring. Specifically, the objective is to generate a time-varying range-vs-angle map indicating the locations of moving targets without confusing NLOS ghost returns due to multipath scattering. Given accurate motion mapping, various motion classification methods can then be applied to each target.

### 1.1. Relation to prior work

MIMO systems offer the flexibility for designing both the transmit and receive beampatterns [8], which have been successfully used for various applications including OTHR [3, 4] and GMTI [5–7]. In [9–11], MIMO systems are used to detect moving targets for improved resolutions. In this paper, we use a MIMO RF probe for wide-area indoor motion monitoring, which has not been well-studied in previous works. This paper also includes real RF experimental results with comparison to traditional SIMO processing, and analysis using the bi-directional beampattern and bi-directional spectrum of the scene.

## 2. SIGNAL MODEL

Consider a continuous-wave MIMO RF probe operating at center frequency  $f_c$  with  $K$  transmit channels and  $N$  receive channels. Without loss of generality, assume that the transmit and receive arrays are collocated 1D uniform linear arrays with inter-element spacing  $d_t$  and  $d_r$ , respectively. For each transmit channel, the transmitted pulse train consists of  $M$  linear frequency modulated (LFM) chirps with pulse repetition interval  $T_r$ . Assume a plane-wave signal which is transmitted at angle  $\phi_t$ , Doppler shifted by  $f_d$ , and received at angle  $\phi_r$ . After pulse compression and range-gating, the signal of the  $m$ -th pulse at the  $n$ -th receive channel from the  $k$ -th transmit channel is given by [7],

$$z_{nk}(m) = \alpha e^{j2\pi f_d m T_r} e^{-j2\pi \frac{f_c}{c} n d_r \sin \phi_r} e^{-j2\pi \frac{f_c}{c} k d_t \sin \phi_t} \quad (1)$$

where  $\alpha$  is a complex amplitude and  $c$  is the speed of propagation. At the  $m$ -th pulse, the signal components in (1) of all

$n$ 's and  $k$ 's form a  $N \times K$  matrix given by

$$\mathbf{Z}(m) = \begin{bmatrix} z_{0\ 0}(m) & \cdots & z_{0\ K-1}(m) \\ z_{1\ 0}(m) & \cdots & z_{1\ K-1}(m) \\ \vdots & \ddots & \vdots \\ z_{N-1\ 0}(m) & \cdots & z_{N-1\ K-1}(m) \end{bmatrix} \quad (2)$$

The signal snapshot  $\mathbf{z}$  is defined as

$$\mathbf{z}(m) = \text{vec}\{\mathbf{Z}(m)\} \quad (3)$$

The vector  $\mathbf{z}(m) \in \mathcal{C}^{NK}$  given in (3) is proportional to the bi-directional wavefront  $\mathbf{v}(\phi_t, \phi_r)$ , which is the Kronecker product of the transmit wavefront  $\mathbf{v}_t(\phi_t)$  and the receive wavefront  $\mathbf{v}_r(\phi_r)$ ,

$$\mathbf{v}(\phi_t, \phi_r) = \mathbf{v}_t(\phi_t) \otimes \mathbf{v}_r(\phi_r) \quad (4)$$

where

$$\begin{aligned} \mathbf{v}_t(\phi) &= \left[ 1, e^{-j2\pi \frac{f_c}{c} d_t \sin \phi}, \dots, e^{-j2\pi \frac{f_c}{c} (K-1) d_t \sin \phi} \right]^T \\ \mathbf{v}_r(\phi) &= \left[ 1, e^{-j2\pi \frac{f_c}{c} d_r \sin \phi}, \dots, e^{-j2\pi \frac{f_c}{c} (N-1) d_r \sin \phi} \right]^T \end{aligned} \quad (5)$$

In an indoor environment, the total return includes direct-path signals  $\mathbf{s}_i$ , multipath returns  $\mathbf{p}_i$ , clutter return  $\mathbf{c}$ , and noise  $\mathbf{n}$ . At each range bin, the returned signal of the  $m$ -th pulse is given by

$$\mathbf{x}(m) = \sum_{i \in \mathcal{I}_s} \mathbf{s}_i(m) + \sum_{i \in \mathcal{I}_p} \mathbf{p}_i(m) + \mathbf{c}(m) + \mathbf{n}(m) \quad (6)$$

where  $\mathcal{I}_s$  and  $\mathcal{I}_p$  denote the index sets of direct-path and multipath returns, respectively. The direct-path signal  $\mathbf{s}_i$  has identical DoD and DoA, thus can be modeled as

$$\mathbf{s}_i(m) = \alpha_{si} e^{j2\pi f_{si} m T_r} \mathbf{v}(\phi_i, \phi_i) \quad (7)$$

The multipath return  $\mathbf{p}_i$  can have arbitrary DoD and DoA, which is given by

$$\mathbf{p}_i(m) = \alpha_{pi} e^{j2\pi f_{pi} m T_r} \mathbf{v}(\phi_{ti}, \phi_{ri}) \quad (8)$$

The clutter is extended to all angles, but its return is repeated over pulses,

$$\mathbf{c}(m) = \iint_{\phi_t, \phi_r} \alpha(\phi_t, \phi_r) \mathbf{v}(\phi_t, \phi_r) d\phi_t d\phi_r \quad (9)$$

The noise is assumed to be uncorrelated among all transmit and receive channels, so its covariance matrix is given by

$$\mathbf{R}_n = \text{E}[\mathbf{nn}^H] = \sigma_n^2 \mathbf{I}_{NK} \quad (10)$$

where  $\mathbf{I}_{NK}$  is an identity matrix of size  $NK \times NK$ .

### 3. INDOOR MOTION MAPPING

For wide-area indoor motion monitoring, a time-varying range-vs-angle map indicating the locations of moving targets is generated using a MIMO RF probe. The processing flow includes 4 steps: pulse compression, clutter removal, bi-directional MIMO beamforming, and motion power estimation.

To locate moving targets in range, pulse compression is applied to the fast-time samples. In this paper, stretch processing is used with LFM chirps to sidestep the requirement of high-rate samplers, and pulse compression is implemented using FFT. After pulse compression, the clutter return at each range bin is removed by highpass filtering the slow-time samples in each channel. Let  $x_{nk}(m)$  denote the slow-time sequence at the  $n$ -th receive channel from the  $k$ -th transmit channel, the filter output  $y_{nk}(m)$  is given by

$$y_{nk}(m) = \sum_{l=0}^{M-1} x_{nk}(l) h(m-l) \quad (11)$$

where  $h(m)$  is the impulse response of a zero-phase highpass filter. After clutter removal, the clutter-free signal in (11) of all transmit and receive channels are put into a vector  $\mathbf{y}(m)$  the same way as in (3). To locate moving targets in angle,  $\mathbf{y}(m)$  is beamformed using weights  $\mathbf{w}(\theta) = \mathbf{v}(\theta, \theta)$ ,

$$\begin{aligned} bf(m) &= \mathbf{w}(\theta)^H \mathbf{y}(m) \\ &= \mathbf{v}(\theta, \theta)^H \mathbf{y}(m) \end{aligned} \quad (12)$$

where  $\theta$  is the beamformer look direction and  $\mathbf{v}(\theta, \theta)$  is the bi-directional wavefront defined in (4) with identical DoD and DoA. The beamformer given in (12) essentially correlates the signal snapshot with the direct-path wavefront, which can be regarded as a spatial matched filter. Finally, the motion power is estimated as the sum of powers at all non-zero Doppler frequencies in the beamformed slow-time sequence, which is equivalent to the power of  $bf(m)$  since the clutter return (zero Doppler) has been removed,

$$P = \sum_{m=0}^{M-1} |bf(m)|^2 \quad (13)$$

The motion power is estimated at each range and angle bin for every coherent processing interval (CPI), and a time-varying range-vs-angle map is obtained.

To analyze the behavior of bi-directional MIMO beamforming, the bi-directional beampattern of weights  $\mathbf{w}(\theta)$  is defined as [12],

$$S(\phi_t, \phi_r) = |\mathbf{w}(\theta)^H \mathbf{v}(\phi_t, \phi_r)|^2 \quad (14)$$

MIMO processing can be regarded as a spatial filter with a response characterized by the beampattern. Fig. 1 shows a

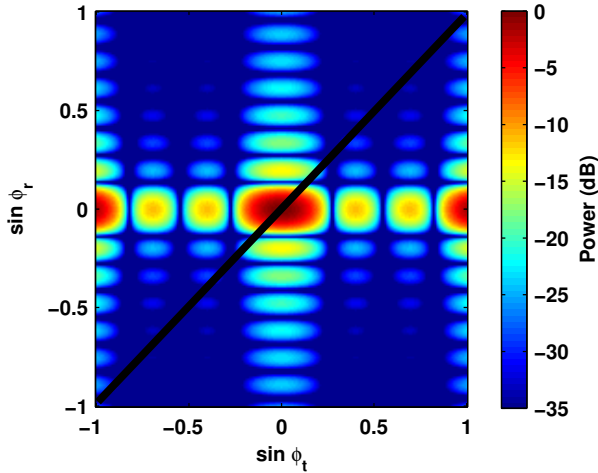


**Fig. 1.** Bi-directional beampattern with a look direction at broadside. The beampattern is simulated with non-adaptive weights and omnidirectional antennas.

bi-directional beampattern with a look direction at broadside. For the MIMO RF probe used in this paper, the transmit channels are separated by about twice the Nyquist spacing. As a consequence, there are grating lobes along the  $\phi_t$  dimension. The gain of using an inter-element spacing larger than half-wavelength is a narrower mainlobe, and the grating lobe issue can be handled by using directional antennas. The sidelobe levels on the diagonal line ( $\phi_t = \phi_r$ ) are lower than those of the transmit or receive beampatterns (horizontal or vertical slices of the bi-directional beampattern). MIMO processing suppresses sidelobes and mitigates multipath by only considering the responses on the diagonal line, which correspond to returns with identical DoD and DoA.

The bi-directional spectrum is also defined for analyzing sidelobes and multipath, which is given by [12],

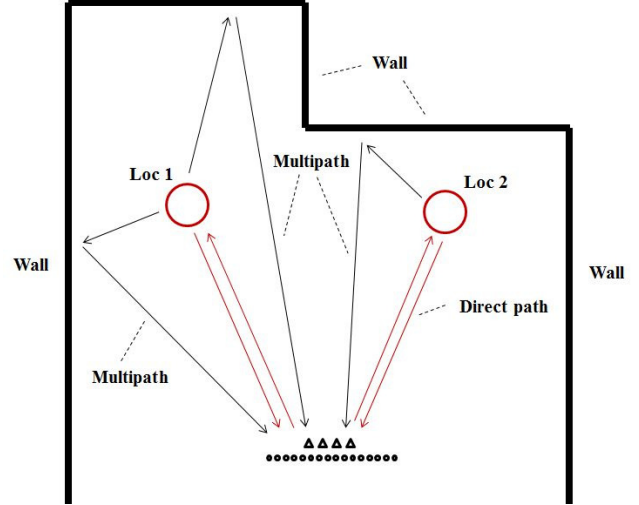
$$\hat{S}(\phi_t, \phi_r) = |\mathbf{v}(\phi_t, \phi_r)^H \hat{\mathbf{v}}|^2 \quad (15)$$

where  $\hat{\mathbf{v}}$  is an estimated snapshot at a certain range and pulse.

## 4. RESULTS AND ANALYSIS

### 4.1. Experiment setup

To validate the feasibility of a MIMO RF probe for indoor motion monitoring, real data are collected in a laboratory environment. The MIMO RF probe used in this paper has 4 transmit channels and 16 receive channels, operating at a center frequency of 2.4 GHz. The LFM chirp has a bandwidth of 600 MHz and the pulse train has a pulse repetition frequency of 100 Hz. The CPI is chosen to be 1.0 s, which contains 100 pulses. The transmit array is uniformly spaced by 11.43 cm (about twice the Nyquist spacing) and the receive array is uniformly spaced by 5.715 cm.



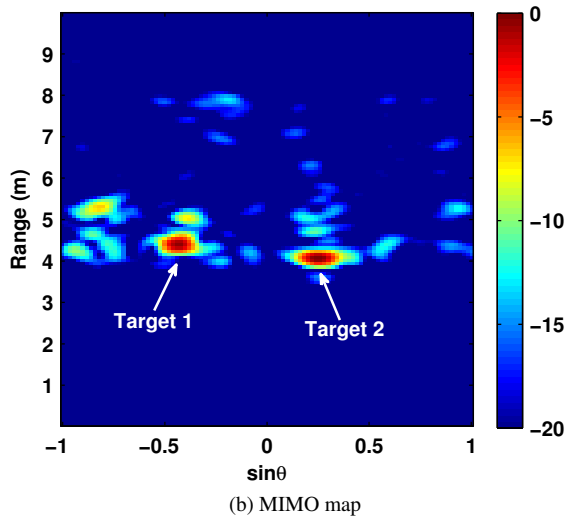
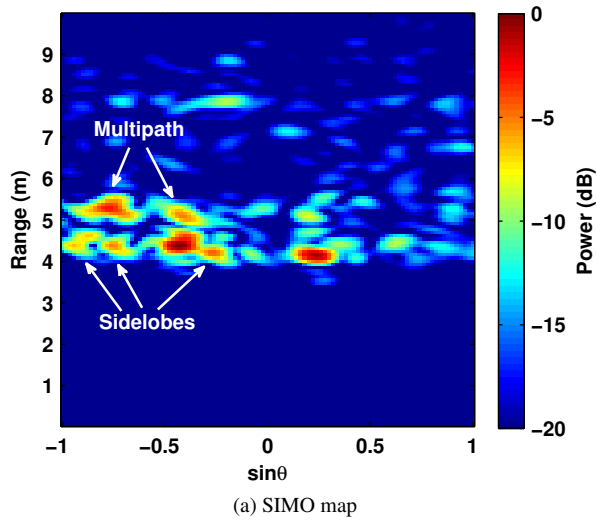
**Fig. 2.** Experiment geometry. The transmit and receive arrays are collocated in the horizontal plane. Two moving locations are about 4 m away from the phase center at different angles.

Fig. 2 shows the geometry of the RF probe location, the motion locations, and the indoor environment. The two red circles, namely “Loc 1” and “Loc 2”, represent the locations where the target stands in each experiment. Two datasets are recorded when the target is moving at “Loc 1” and “Loc 2”, respectively. Each dataset is recorded for 10 s, and the two datasets are combined to obtain a simulated multiple-target return.

### 4.2. Motion map and bi-directional spectrum

Fig. 3 shows the motion maps obtained via SIMO and MIMO processing, respectively. In both maps, the two strongest peaks represent the true moving targets and their locations. It can be seen in Fig. 3 (a) that there are still several strong peaks other than the two targets. These peaks are in fact sidelobes and multipath (ghost returns). Sidelobes exist at the same range as the moving targets, while multipath exist at further ranges. Observe that the MIMO map shown in Fig. 3 (b) does not exhibit the sidelobes or multipath evident in the SIMO map, which demonstrate the ability of bi-directional MIMO beamforming for sidelobe suppression and multipath mitigation.

To analyze the behavior of MIMO processing, the bi-directional spectra defined in (15) at the target range and the multipath range are presented here. Fig. 4 shows the spectrum at the target range. The two peaks on the diagonal line represent the angles of the two direct-path targets, which match the angles in both motion maps. For SIMO systems, only the receive angle can be estimated. Therefore, the output of SIMO processing is equivalent to the vertical slices of the bi-directional spectrum. Consequently, the sidelobe peaks marked in black circles will exist after beam-



**Fig. 3.** Motion maps obtained using (a) traditional SIMO processing and (b) MIMO processing.

forming, corresponding to the three sidelobes at the same range as the moving targets, as annotated in Fig. 3 (a). In contrast, bi-directional MIMO beamforming only considers the responses on the diagonal line, which suppresses those sidelobes, as shown in Fig. 3 (b).

Fig. 5 shows the spectrum at the multipath range. The peaks marked in black rectangles represent the two multipath returns annotated in the SIMO map. Since the two ghost returns have different DoD than DoA (not on the diagonal line), they are successfully mitigated by MIMO processing. Note that there is a transmit sidelobe on the diagonal line at the same receive angle as the stronger multipath, which exists in the MIMO map. However, this ghost return is much weaker compared to the one at the same location in the SIMO map, since it is just a sidelobe of the multipath.

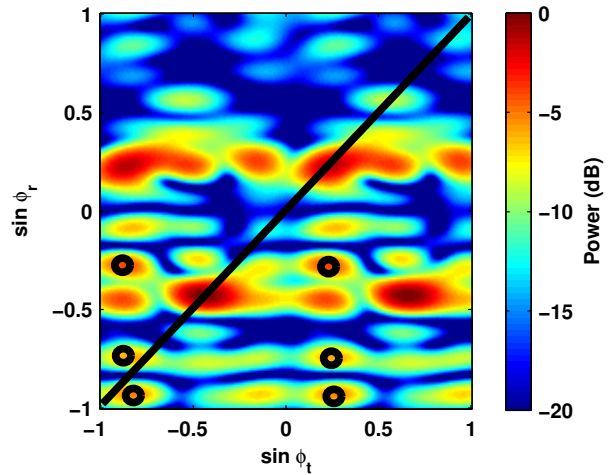


**Fig. 4.** Bi-directional spectrum at target range.

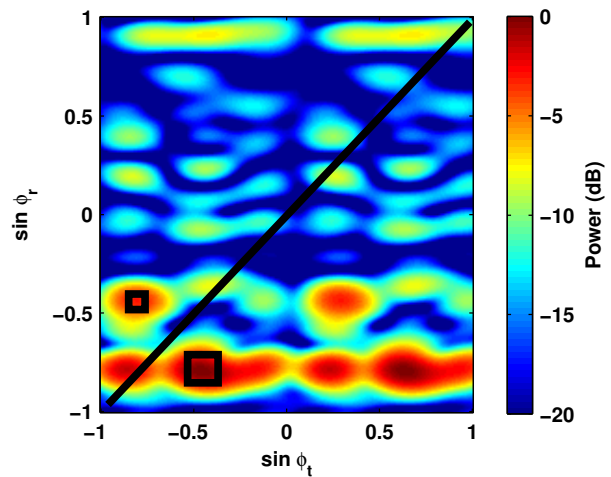


**Fig. 5.** Bi-directional spectrum at multipath range.

## 5. CONCLUSION AND FUTURE WORK

A RF-based approach is proposed for simultaneous monitoring of multiple moving targets in indoor environments. The range and angle of motions are obtained using a MIMO RF probe. Bi-directional MIMO beamforming is used for sidelobe suppression and multipath mitigation. Real data experiments validate the feasibility of the proposed method. In the future work, methods for human motion classification will be exploited using the real data collected from the system.

## 6. ACKNOWLEDGMENT

This work is supported by the Information Initiative at Duke (i.i.D.).

## 7. REFERENCES

- [1] T. B. Moeslund, A. Hilton, and V. Kruger, "A survey of advances in vision-based human motion capture and analysis," *J. Computer Vision and Image Understanding*, vol. 104, pp. 90–126, Nov. 2006.
- [2] Y. Kim and H. Ling, "Human activity classification based on micro-doppler signatures using a support vector machine," *IEEE Trans. Geosci. Remote Sens.*, vol. 47, pp. 1328–1337, May 2009.
- [3] G. J. Frazer, Y. I. Abramovich, and B. A. Johnson, "Multiple-input multiple-output over-the-horizon radar: experimental results," *IET radar, sonar & navigation*, vol. 3, pp. 290–303, Aug. 2009.
- [4] Y. I. Abramovich, G. J. Frazer, and B. A. Johnson, "Noncausal adaptive spatial clutter mitigation in monostatic MIMO radar: Fundamental limitations," *IEEE J. Sel. Topics Signal Process.*, vol. 4, pp. 40–54, Feb. 2010.
- [5] D. W. Bliss, K. W. Forsythe, S. K. Davis, G. S. Fawcett, D. J. Rabideau, L. L. Horowitz, and S. Kraut, "GMTI MIMO radar," in *Int. Waveform Diversity and Design Conf.*, 2009, pp. 118–122.
- [6] G. Hickman and J. L. Krolik, "MIMO GMTI radar with multipath clutter suppression," in *IEEE Sensor Array and Multichannel Signal Processing Workshop*, 2010, pp. 65–68.
- [7] J. Yu and J. Krolik, "MIMO multipath clutter mitigation for GMTI automotive radar in urban environments," in *IET Int. Conf. Radar Systems*, 2012, pp. 1–5.
- [8] J. Li and P. Stoica, "MIMO radar with colocated antennas," *IEEE Signal Processing Mag.*, vol. 24, pp. 106–114, Sept. 2007.
- [9] I. Bekkerman and J. Tabrikian, "Target detection and localization using MIMO radars and sonars," *IEEE Trans. Signal Process.*, vol. 54, pp. 3873–3883, Oct. 2006.
- [10] Q. He, N. H. Lehmann, R. S. Blum, and A. M. Haimovich, "MIMO radar moving target detection in homogeneous clutter," *IEEE Trans. Aerosp. Electron. Syst.*, vol. 46, pp. 1290–1301, July 2010.
- [11] X. P. Masbernat, M. G. Amin, F. Ahmad, and C. Ioana, "An MIMO-MTI approach for through-the-wall radar imaging applications," in *Int. Waveform Diversity and Design Conf.*, 2010, pp. 188–192.
- [12] J. Yu and J. Krolik, "MIMO adaptive beamforming for non-separable multipath clutter mitigation," *IEEE Trans. Aerosp. Electron. Syst.*, submitted for publication.